Vibration Energy Harvesting IC Design with Incorporation of Two Maximum Power Point Tracking Methods

Jinhua Wang, Jiayu Li, and Dong Sam Ha
Multifunctional Integrated Circuits and Systems (MICS) Group
Bradley Department of Electrical and Computer Engineering
Virginia Tech, Blacksburg, Virginia, 24061, USA
Email: {wjinhua6, jli4, ha}@vt.edu

Abstract—The proposed circuit aims to harvest energy from vibration with piezoelectric transducers (PZTs). As the operating conditions of a PZT change, the PZT impedance also changes. Therefore, maximum power point tracking (MPPT) is required. The optimal fraction k_{opt} is the ratio of the load voltage to the source voltage at the maximum power point (MPP). The fractional open-circuit voltage (FOCV) method regulates the load voltage to operate at the MPP for a given k_{opt} . The P&O method obtains k_{opt} first and then regulates the load voltage. The proposed MPPT method integrates the FOCV and P&O methods to take advantages of the two methods. The proposed circuit is designed in TSMC BCDMOS 0.18 μ m technology. The post-layout simulations verify operation of the proposed circuit.

Keywords— energy harvesting, maximum power point tracking (MPPT), fractional open-circuit voltage (FOCV), perturb and observe (P&O), vibration energy

I. INTRODUCTION

The demand for self-powered devices such as wireless IoT devices, wireless sensor nodes (WSNs), and wearable devices, has increased rapidly in the past decades. Harvesting energy from ambient energy sources such as vibration, temperature gradient, RF and AC powerlines, is a promising solution to power such devices [1]-[4].

A piezoelectric transducer (PZT) is often used to harvest vibration energy, and a typical PZT can harvest energy ranging from μW to mW [5]-[7]. As the operating conditions of the PZT change, the PZT impedance also changes. Hence, maximum power point tracking (MPPT) is necessary to operate the PZT at the maximum power point (MPP) under varying operating conditions. Note that the maximum energy is extracted from the PZT and delivered to the load at the MPP. A key requirement for MPPT circuits for PZTs is low power dissipation. Various MPPT methods for PZTs were investigated [8]-[10]. Two common MPPT methods for PZTs are Fractional Open Circuit Voltage (FOCV) and Perturb and Observe (P&O). The FOCV method is relatively simple to result in low circuit complexity and hence low power dissipation [11]-[13]. One shortcoming of the FOCV method is that it does not guarantee to operate at the MPP, especially under varying operating conditions, resulting low efficiency. In contrast, the P&O method ensures to operate at the MPP ideally [10], [13]-[15]. However, the method incurs high circuit complexity, resulting in high power dissipation.

A traditional energy harvesting circuit usually adopts two DC-DC converters in series: the first one for MPPT and the second one for load voltage regulation [6]. Two converters incur large power dissipation and hence low efficiency. The dualinput dual-output (DIDO) topology needs only one DC-DC converter and is widely adopted [10]-[12]. A battery is used for a DIDO circuit to regulate the load voltage as well as to store excessive energy. The battery also supplements energy to the load if the PZT does not generate enough energy. The proposed circuit adopts the DIDO topology and integrates both FOCV and P&O methods to exploit advantages of the two methods.

This paper is organized as follows. Section II reviews a PZT model and two traditional MPPT schemes. Section III presents the proposed MPPT circuit. Section IV shows the layout and post-layout simulation results. Section V concludes the paper.

II. PRELIMINARIES

A. PZT Model and Impedance Characteristics

Fig. 1 shows an equivalent circuit model for a PZT and its impedance curve [16]. The internal impedance behaves mostly capacitive outside of the resonant frequency region, and the maximum power is extracted from a PZT at the resonant frequency. The magnitude of the PZT impedance changes as the operating frequency of the PZT changes, and the magnitude is somewhat sensitive at the resonant frequency range.

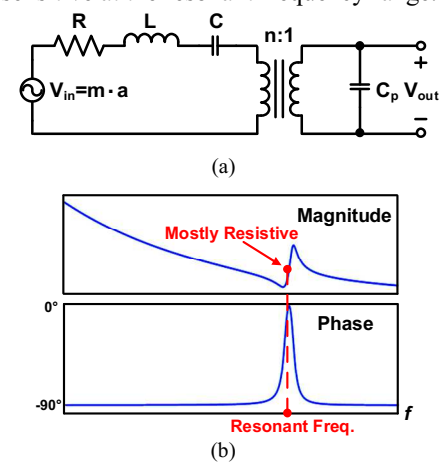


Fig. 1. PZT (a) equivalent circuit model, (b) impedance curve.

Fig. 2 shows a PZT with a resistive load R_L . The maximum power is delivered from the PZT to the load provided $R_L = |Z_S|$, where Z_S is the internal impedance of the PZT [16]. The ratio V_L/V_S under $R_L = |Z_S|$ is

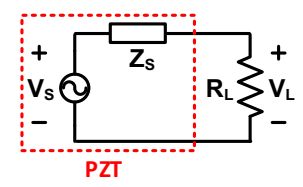


Fig. 2. PZT with a resistive load R_L.

called *optimal fraction* k_{opt} . Note that the k_{opt} is 0.5 for the purely reistive Z_S and is close to 0.5 at the resonant frequency region. As the operating frequency of the PZT changes, Z_S changes. Hence, R_L should be adjusted accordingly to operate at the MPP, resulting in change of the k_{opt} . Note that the source voltage V_S is also called open circuit voltage V_{oc} in this paper.

B. Maximum Power Point Tracking (MPPT)

In general, the fraction k is expressed as below.

$$V_L = kV_S = kV_{oc} \tag{1}$$

where V_L is the load voltage and V_{oc} is the open circuit voltage or the source voltage without being connected to the load. An MPPT method monitors the operating conditions of the PZT and adjusts V_L accordingly to operate at the MPP. In practice, an MPPT circuit adjusts the load resistance R_L to maintain the optimal fraction k_{opt} . The FOCV method relies on the k_{opt} obtained for a certain MPP, and most existing FOCV circuits consider a fixed k_{opt} . Since the k_{opt} is given for the FOCV method, it does not require to measure the power delivered to the load or search for the MPP, resulting in low power dissipation of the circuit. However, the actual k_{opt} varies as the operating conditions such as the operating frequency of a PZT change. Therefore, the FOCV method does not ensure operation of the energy harvesting circuit at the MPP under varying operating conditions. It leads to low efficiency of the FOCV method.

In contrast, the P&O method searches for the k_{opt} first through measurement of the power delivered to the load and then aims to maintain the k_{opt} . The P&O method adopted for the proposed method obtains the k_{opt} as follows. Let k(n) be the kvalue at the current clock cycle n. It perturbs or increases (decreases) k(n) by δ for the next cycle (n+1) and measures the power. If the power for the cycle (n+1) is larger than that of the cycle n, it increases (decreases) k(n+1) again by δ for the next cycle (n+2). If the power is smaller, it switches the direction of the perturbation. The P&O method ensures to operate at the MPP ideally even if the operation conditions change. A shortcoming of the P&O method is high circuit complexity due to the need to measure the power, resulting high power dissipation of the MPPT circuit. The proposed method integrates the FOCV and P&O methods to take the advantages of both methods.

III. PROPOSED MPPT METHOD

This section presents the overview of the proposed circuit and explains integration of the two MPPT methods, FOCV and P&O.

A. System Architecture

Fig. 3 shows the overall circuit with a 2P3S converter and its three major building blocks. The rectified PZT voltage V_{rect} is

the load voltage V_L under the closed SW₁ and the open circuit voltage V_{oc} under the open SW₁. The maximum voltage V_{oc} is 32 V for the circuit, and the maximum input current to the converter is 25 mA. The "I/O Monitoring & Mode Selection" block generates switching signals for the three switches, SW₁, SW₂, and SW₃. Constant On-time Pulse Skipping Modulation (COT-PSM) is adopted for the converter [15].The turn-on time of the switching signals for the switches is fixed and a switching signal or pulse could be skipped for the COT-PSM.The MPPT block consists of two sub-block, FOCV and P&O, and each block is controlled by the separated clock, CLK_{FOCV} and $CLK_{Observe}$.

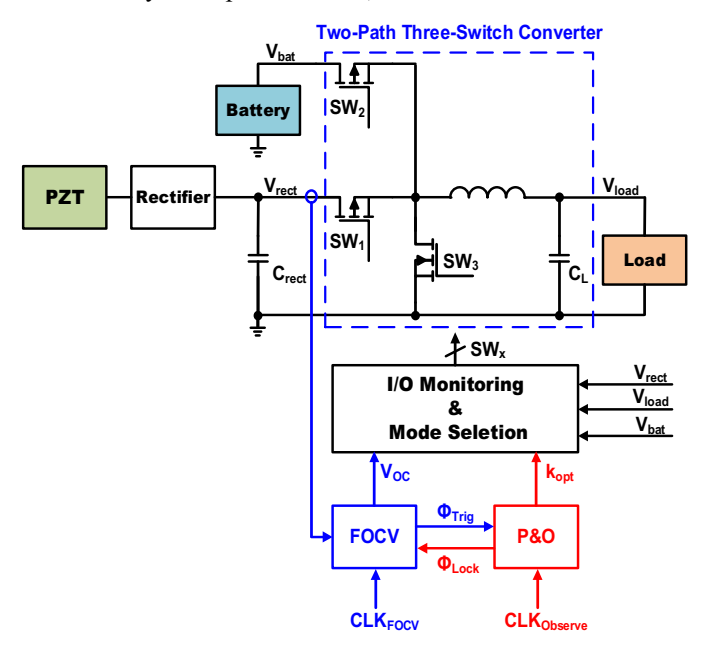


Fig. 3. Proposed circuit with a two-path three-switch (2P3S) converter.

The top block in Fig. 3 is a two-path three-switch (2P3S) converter proposed in [11], which is based on the DIDO topology. The 2P3S converter can operate in three different operation modes. The first mode is the "Harvest" mode, in which energy is harvested from the PZT and transferred to the load. Two switches, SW₁ and SW₃, with the associated inductor, form a buck converter, while SW₂ is open. The second mode is the "Supplement" mode, in which the battery provides energy to the load. The buck converter composed of SW₂ and SW₃ transfers the energy, while SW₁ is open. The last mode is the "Recycle" mode. The excessive energy stored at the load capacitor C_L is transferred to the battery by a boost converter composed of SW₃ and SW₂, while SW₁ is open.

Fig. 4 shows the main part of the "I/O Monitoring & Mode Selection" block consisting of an on-time generator, an off-time generator, and gate drives. The on-time generator generates pulses with a fixed on-time period, and the off-time generator generates pulses with a fixed off-time period at the falling edge of the pulse. A 2-bit signal, S_1S_0 , sets the operation mode (00 for *Harvest*, 01 for *Supplement*, and 10 for *Recycle*) of the 2P3S converter through monitoring of the three voltages, V_{rect} , V_{load} , and V_{bat} . For example, if V_{rect} is high and V_{load} is low, the EN signal goes high, and the on-time pulse is applied to SW_1 of the buck converter in Fig. 3 and the off-time pulse is applied to SW_3 . SW_2 is 0 to turn off the switch . For details, refer to [15], [17].

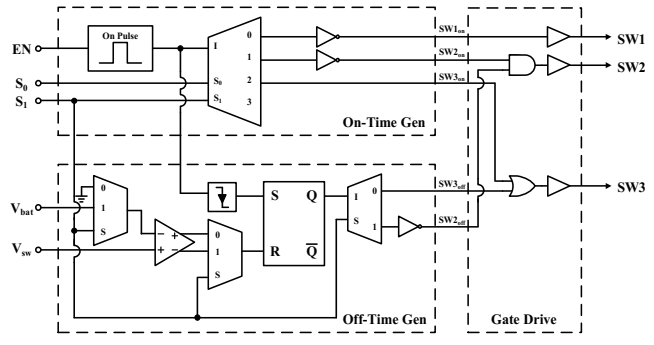
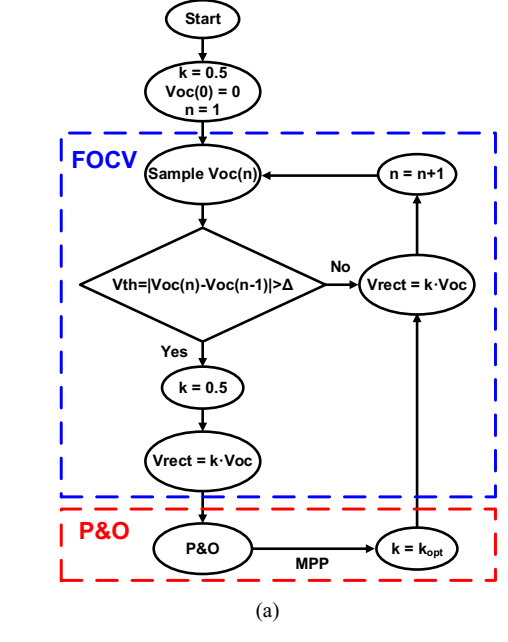


Fig. 4. I/O Monitoring & Mode Selection block.

B. Overview of Proposed MPPT Method



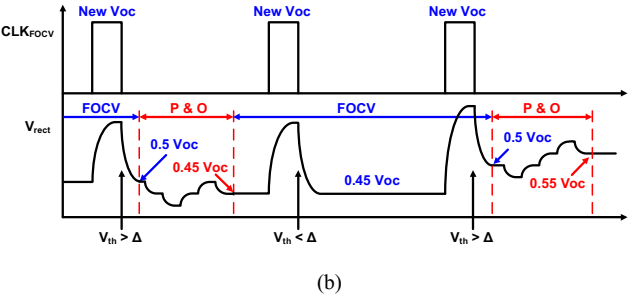


Fig. 5. Proposed MPPT method (a) flowchart, (b) expected waveforms.

The proposed MPPT method integrates two MPPT methods, FOCV and P&O, to operate at the MPP region with low power dissipation. Fig. 5(a) shows the flowchart of the proposed MPPT method. When the energy harvesting circuit wakes up from the sleep mode, it enters the FOCV mode with k = 0.5. It compares two consecutive samples of the open circuit voltage, $V_{oc}(n)$ and $V_{oc}(n-1)$. If the difference of the two samples denoted as V_{th} is greater than a preset value Δ as shown in (2), it implies that the PZT operating condition is changed, and requires a new optimal fraction k_{opt} .

$$V_{th} = |V_{oc}(n) - V_{oc}(n-1)| > \Delta$$
 (2)

Therefore, the proposed method enters to the P&O mode and obtains the new k_{opt} for the new MPP and exits the P&O mode. A new open circuit voltage is sampled in the FOCV mode and compared with the previous one. Now, suppose that the difference V_{th} is smaller than Δ , implying little change of the operating condition and hence the current k_{opt} is still valid. It uses the current k_{opt} to regulate the rectified voltage V_{rect} with load to $k_{opt} \times V_{oc}(n)$, equivalently speaking, to operate at the MPP. The regulation of the rectified voltage is performed through pulse skipping modulation. If V_{rect} is greater than $k_{opt} \times V_{oc}(n)$, a switching signal is applied to the buck converter in the harvest mode, which reduces V_{rect} . If V_{rect} is smaller, the switching pulse is skipped. The harvested energy is stored in the input capacitor C_{rect} in Fig. 3, resulting in an increase of V_{rect} .

Fig. 5(b) shows the waveforms of the rectified voltage V_{rect} for the proposed MPPT method. When the clock CLK_{FOCV} is high, the rectified voltage V_{rect} is disconnected from the load, and V_{rect} rises rapidly toward the open circuit voltage $V_{oc}(1)$. As it exits the FOCV mode, $V_{rect} = 0.5 V_{oc}(1)$. As the difference $|V_{oc}(1) - V_{oc}(0)|$ is greater than Δ , it enters the P&O mode. When it exits the P&O mode, $V_{rect} = 0.45 V_{oc}(1)$, implying the new $k_{opt} = 0.45$. The next $V_{oc}(2)$ is the same as or close to $V_{oc}(1)$, and it implies the operation condition has not changed. The circuit remains in the FOCV mode with the same $k_{opt} = 0.45$. The third sample $V_{oc}(3)$ is far larger than $V_{oc}(2)$. It enters the P&O mode and obtains the new $k_{opt} = 0.55$.

C. FOCV Mode

Fig. 6(a) shows the FOCV decision block. Two identical sample and hold circuits take turns to sample the open circuit voltage V_{oc} and store the sampled value in the associated capacitor. The capacitor size is chosen large enough, so that it is able to hold a sampled value until the next sample. At the same time, the capacitor is small enough to charge up to V_{oc} during the on-time of the associated switch.

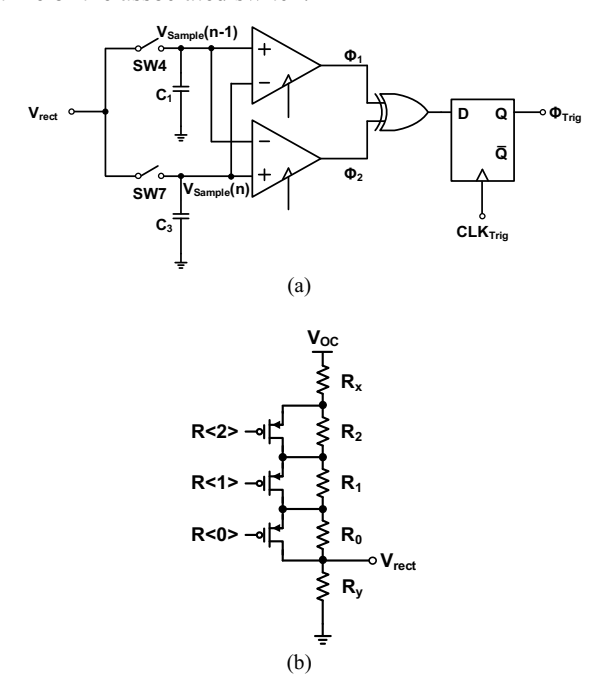


Fig. 6. (a) FOCV decision block, (b) 3-bit resistive ladder.

The sampling clock CLK_{FOCV} for the FOCV block in Fig. 3 has the frequency of 0.1 Hz or the clock period of 10 second, and the on-time period of 50 ms. The sampling clock for SW₇ follows the sampling clock CLK_{FOCV} for SW₄ with the delay of 5 seconds. When the sampling clock pulse is on, the signal SW1 in Fig. 4 is 0, which turns off the switch SW₁ of the 2P3S converter in Fig. 3. It implies the PZT with the rectifier is disconnected from the load, and V_{rect} becomes the open circuit voltage V_{oc} . During the sampling period, the battery supplies energy to the load.

Two *hysteresis* comparators along with an XOR gate in Fig. 6(a) determine whether the voltage difference of two consecutive samples is greater than the preset value Δ or not. The two sampled voltages are applied to the opposite inputs of the two comparators as shown in the figure. If the difference of the two voltage is greater than Δ , the comparator outputs $\Phi_1\Phi_2$ =10 or 01, resulting the XOR gate output being logic 1. It sets the DFF output Φ_{Trig} to logic 1, which makes the MPPT block to leave the FOCV mode and enter to the P&O mode. If the difference of the two sampled voltage is less than Δ , the comparator outputs $\Phi_1\Phi_2=00$, resulting the XOR gate output being logic 0. The MPPT block remains in the FOCV mode. Finally, the preset value Δ is controlled by the hysteresis of the comparators, and it is set to 0.1 V by the external voltage for the proposed design.

D. P&O Mode

The proposed MPPT method obtains the optimal fraction k_{opt} in the P&O mode. It perturbs the fraction k and checks whether the power delivered to the load increases or not. The resistive ladder shown in Fig. 6(b) and a 3-bit up/down counter R<2:0> are used to perturb k. The resistances of the ladder are chosen as $R_1 = 2R_0$ and $R_2 = 4R_0$. The fraction k is expressed as follows.

$$k \equiv \frac{V_{rect}}{V_{OC}} = \frac{R_y}{[R(0) + 2R(1) + 4R(2)]R_0 + R_x + R_y}$$
(3)

The 3-bit counter R<2:0> is used to perturb k and sets a k value out of 8 possible ones. Note that k is the largest for R<2:0> = 000 and smallest for R<2:0> = 111.

To find the optimal fraction k_{opt} , the counter increments or increments by 1 and compares the power delivered to the load. If the power increases, the counter keeps on incrementing or decrementing in the same direction. If the power decreases, then the k value set by the previous counter value is the optimal. For example, suppose the initial value of R<2:0> is 011. The counter is decremented to 010 or k increases by a certain amount. If the power delivered to the load increases after the decrement, the counter is decremented again to 001 in the next system clock cycle. Now, suppose the power is decreased. Then the optimal fraction k_{opt} is the one set by the previous counter value or R<2:0> = 010. In practice, the proposed circuit sets the optimal counter value if direction of the power changes two times, which makes the circuit operation more reliable.

The P&O mode requires the comparison of power delivered to the load before and after a perturbation of k, and a current sensor for power measurement dissipates power. When a buck converter operates in discontinuous conduction mode (DCM) with a constant on-time switching signal, the off-time period of the switching signal can be measured to approximate the power

delivered to the load [10], [15]. The measurement of the off-time period eliminates a current sensor to save power. Note that the 2P3S converter in Fig. 3 is configured as a buck converter in the P&O mode, the proposed MPPT circuit adopts the method proposed in [10], [15], which can also be applicable to the COT-PSM adopted for the proposed circuit.

IV. LAYOUT AND SIMULATION RESULTS

A. Layout

The proposed circuit is designed and laid out in TSMC 0.18 μ m BCDMOS technology and taped out for fabrication. Fig. 7 shows the layout. The entire chip size is 3 mm x 1.3 mm with the active die area of 2.5 mm x 1 mm. Most area is occupied by the three power switches due to the large breakdown voltage of 36 V. The rectifier, inductor, input and out capacitors (C_{rect} and C_L) are off-chip.

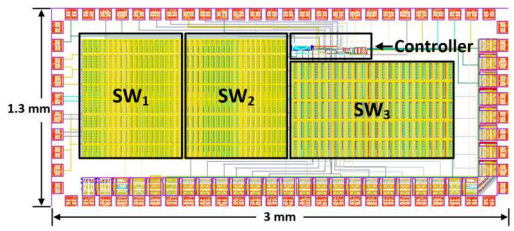


Fig. 7. Layout of the proposed circuit.

B. Simulation Results

Fig. 8 shows post-layout simulations for the proposed MPPT circuit. Fig. 8(a) shows operation of the FOCV decision block in Fig. 6(a). Two capacitors C_1 and C_2 take turns to store sampled voltages, $V_{Sample1}$ and $V_{Sample2}$. According to (2), the difference between the two sampled voltages is greater than the preset value Δ of 100 mV after the first and third clocks. Thus, the signal Φ_{Trig} is triggered to logic 1, and the FOCV mode starts.

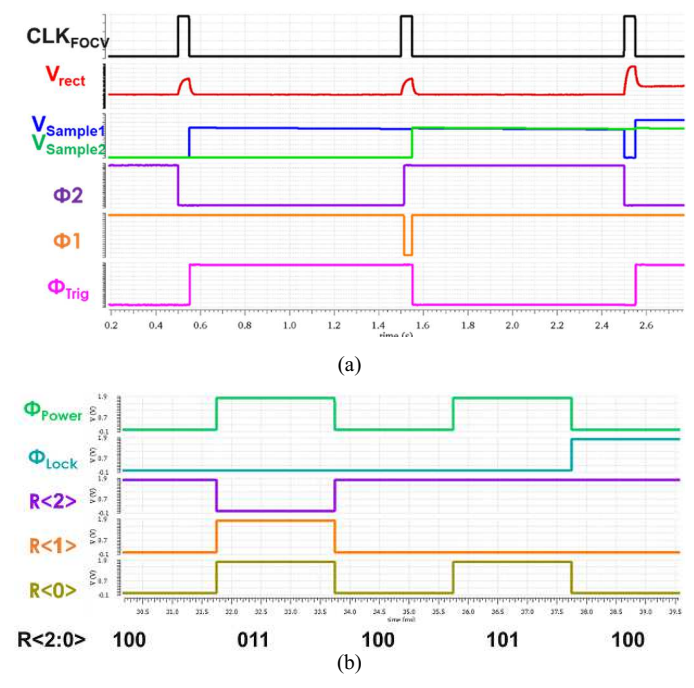


Fig. 8. Simulation results (a) FOCV mode, (b) P&O mode.

Fig. 8(b) shows operation of the circuit in the P&O mode. $\Phi_{Power} = 1$ indicates the power level under the previous k is higher than that of the current k, where k is perturbed by increase/decrease of R<2:0>. As R<2:0> changes from 100 to 011, the power level decreases to set $\Phi_{Power} = 1$. So R<2:0> changes back to 100 in the next cycle, resulting $\Phi_{Power} = 0$ or increase of the power as expected. As the change R<2:0> = 011 \rightarrow 100 increases the power, R<2:0> further increases to 101, resulting $\Phi_{Power} = 1$. As the number of power decrements or the occurrence of $\Phi_{Power} = 1$ is 2, Φ_{Lock} is triggered to lock R<2:0> = 100.

As mentioned in Section III C, the sampling clock pulse *CLK_{FOCV}* in the FOCV mode is 0.1 Hz. It takes too long for post layout simulation of the entire circuit under such a low frequency. We set CLK_{FOCV} to 1 MHz for the purpose of the simulation. Also, the PZT integrated with an off-chip rectifier is modeled as a DC voltage source of 5 V / 0 V with the internal resistance $Z_S = 80 \text{ k}\Omega$ in the simulation, and the load resistance R_L is set to 3 k Ω . The optimal fraction k_{opt} is set to 0.4. Fig. 9 shows the simulation results for one MPPT cycle. The MPPT cycle starts from the FOCV mode. The open circuit voltage V_{oc} or V_{rect} with the disconnected buck converter is sampled at 5 V, and drops to $0.5V_{oc}$. Since the buck converter is disconnected from the source, the mode selection signal S₁S₀ is set to 01 (Supplement mode), and the load is powered by the battery. Then, the circuit enters the P&O mode. S₁S₀ changes to 10 (Recycle mode), and the battery is powered by the load. After the circuit reaches k_{opt} of 0.4, S_1S_0 becomes 00 (*Harvest* mode) and the circuit starts to harvest energy from the source and powers the load. The proposed circuit can harvest 3.63 mW at the MPP or $k_{opt} = 0.4$.

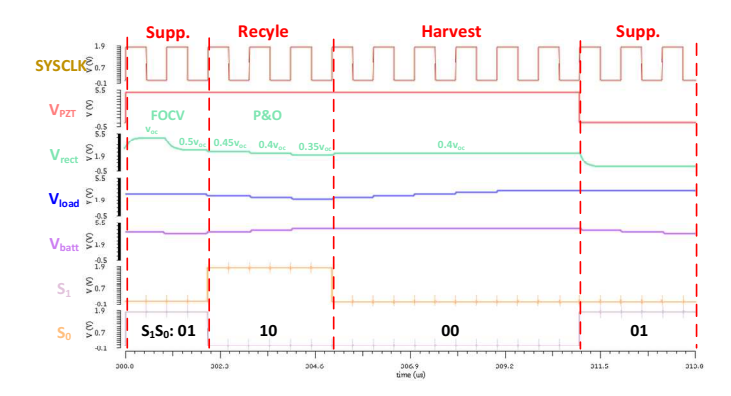


Fig. 9. Post-layout simulation for one MPPT cycle.

V. CONCLUSION

This paper presents a vibration energy harvesting circuit for PZTs. The proposed MPPT method integrates two commonly used MPPT methods, FOCV and P&O, to exploit the advantages of the two methods. The circuit is designed in TSMC 0.18 µm BCDMOS technology and taped out for fabrication. The post-layout simulations verify the operation of the circuit.

ACKNOWLEDGMENT

This research was supported in part by the National Science Foundation Award number 1704176.

REFERENCES

- [1] B. Zhao, J. Wang, W. -H. Liao and J. Liang, "A Bidirectional Energy Conversion Circuit Toward Multifunctional Piezoelectric Energy Harvesting and Vibration Excitation Purposes," in IEEE Transactions on Power Electronics, vol. 36, no. 11, pp. 12889-12897, Nov. 2021.
- [2] J. H. Hyun, L. Huang and D. S. Ha, "Vibration and Thermal Energy Harvesting System for Automobiles with Impedance Matching and Wake-up," 2018 IEEE International Symposium on Circuits and Systems (ISCAS), May 2018.
- [3] R. Reed, F. L. Pour and D. S. Ha, "An Efficient 2.4 GHz Differential Rectenna for Radio Frequency Energy Harvesting," 2020 IEEE 63rd International Midwest Symposium on Circuits and Systems (MWSCAS), pp. 208-212, Aug. 2020.
- [4] J. Wang, J. Kim and D. S. Ha, "Powerline Energy Harvesting Circuit with a Desaturation Controller for a Magnetic Core," 2021 IEEE International Midwest Symposium on Circuits and Systems (MWSCAS), pp. 220-223, Aug. 2021.
- [5] M. Edla, Y. Y. Lim, D. Mikio and R. V. Padilla, "A Single-Stage Rectifier-Less Boost Converter Circuit for Piezoelectric Energy Harvesting Systems," in IEEE Transactions on Energy Conversion, vol. 37, no. 1, pp. 505-514, Mar. 2022.
- [6] F. Dell'Anna et al., "State-of-the-Art Power Management Circuits for Piezoelectric Energy Harvesters," in IEEE Circuits and Systems Magazine, vol. 18, no. 3, pp. 27-48, thirdquarter 2018.
- [7] H. Xia, et al., "Self-Powered Dual-Inductor MI-PSSHI-VDR Interface Circuit for Multi-PZTs Energy Harvesting," in IEEE Transactions on Power Electronics, vol. 37, no. 4, pp. 3753-3762, Apr. 2022.
- [8] L. Wu, X. Do, S. Lee and D. S. Ha, "A Self-Powered and Optimal SSHI Circuit Integrated With an Active Rectifier for Piezoelectric Energy Harvesting," in IEEE Transactions on Circuits and Systems I: Regular Papers, vol. 64, no. 3, pp. 537-549, March 2017.
- [9] S. Uprety and H. Lee, "A 0.65-mW-to-1-W Photovoltaic Energy Harvester With Irradiance-Aware Auto-Configurable Hybrid MPPT Achieving >95% MPPT Efficiency and 2.9-ms FOCV Transient Time," in IEEE Journal of Solid-State Circuits, vol. 56, no. 6, pp. 1827-1836, June 2021.
- [10] S. Bandyopadhyay and A. P. Chandrakasan, "Platform architecture for solar, thermal and vibration energy combining with MPPT and single inductor," 2011 Symposium on VLSI Circuits - Digest of Technical Papers, pp. 238-239, Sept. 2011.
- [11] Y. Wang, Y. Huang, P. Huang, H. Chen and T. Kuo, "A Single-Inductor Dual-Path Three-Switch Converter With Energy-Recycling Technique for Light Energy Harvesting," in IEEE Journal of Solid-State Circuits, vol. 51, no. 11, pp. 2716-2728, Nov. 2016.
- [12] P. Prabhakaran and V. Agarwal, "Novel Four-Port DC-DC Converter for Interfacing Solar PV-Fuel Cell Hybrid Sources With Low-Voltage Bipolar DC Microgrids," in IEEE Journal of Emerging and Selected Topics in Power Electronics, vol. 8, no. 2, pp. 1330-1340, Jun. 2020.
- [13] M. Balato, L. Costanzo, A. Lo Schiavo, M. Vielli, "Optimization of both Perturb & Observe and Open Circuit Voltage MPPT Techniques for Resonant Piezoelectric Vibration Harvesters feeding bridge rectifiers," in Sensors and Actuators A: Physical, vol 178, pp. 85-97, Aug. 2018.
- [14] N. Kong and D. S. Ha, "Low-Power Design of a Self-powered Piezoelectric Energy Harvesting System With Maximum Power Point Tracking," in IEEE Transactions on Power Electronics, vol. 27, no. 5, pp. 2298-2308, May 2012.
- [15] J. Wang, J. Li and D. S. Ha, "Energy Harvesting Circuit for Indoor Light Based on the FOCV and P&O Schemes with an Adaptive Fraction Approach," 2020 IEEE International Symposium on Circuits and Systems (ISCAS), May 2020.
- [16] N. Kong, D.S. Ha, A. Erturk, and D.J. Inman, "Resistive Impedance Matching Circuit for Piezoelectric Energy Harvesting," Journal of Intelligent Material Systems and Structures, Vol. 21, No. 13, pp. 1293 -1302, Sept. 2010.
- [17] J. Li, Vibration Energy Harvesting IC Design with Incorporation of Two Maximum Power Point Tracking Methods, MS thesis, ECE Department, Virginia Tech, 2020.